Quantum percolation and Anderson transition point for transport of a two-state particle

C. M. Chandrashekar[1,*] and Th. Busch[1,†]

[1] *Quantum Systems Unit, Okinawa Institute of Science and Technology, Okinawa 904-0495, Japan*

Quantum percolation describes the problem of a quantum particle moving through a randomly frozen medium. While certain similarities to classical percolation exist, the dynamics of quantum percolation has additional complexity due to the possibility of Anderson localization. Here we show that this strongly influences the percolations threshold by considering a directed two-state quantum walk on a two dimensional space. To do this we determine the Anderson transition point (the quantum equivalent to the classical percolation threshold) for three fundamental lattice geometries (finite square lattice, honeycomb lattice, and nanotube structure) and show that it differs significantly from the classical value and tends towards unity for increasing lattice sizes. Beyond the fundamental interest for understanding the dynamics of a two-state particle on the lattice (network) with disconnected vertices, our study also sheds light on the transport dynamics in various quantum condensed matter systems and the construction of several quantum information processing and communication protocols.

Percolation theory is a mathematical model originally developed to describe the dynamics of particles in random media [1]. Due to its fundamental nature it has since established itself as an area of research on its own right and found numerous applications in diverse fields. These include fluid dynamics, fire propagation, many body system in classical and quantum physics, information theory, dynamics in biological system and in chemical components [2, 3].

The main figure of merit which determines the transport efficiency of a particle in percolation theory is the so-called percolation threshold [4]. To illustrate its meaning in the classical setting, one can consider transport on a square lattice with neighbouring vertices connected with probability p. When $p = 0$, all vertices are disconnected from each other and no path for the particle to move across the lattice exists. With increasing p more and more vertices will be connected and when $p = p_c = 0.5$ the first connection across the full lattice is established.

The corresponding problem of percolation of a quantum particle differs from the classical setting in that it contains an additional degree of freedom. In a disordered system the interference of the different phases accumulated along different routes during the evolution can lead to the particle's wave function becoming exponentially localized. This process known as Anderson localisation [5–7] and has recently been observed in different disordered systems [8–10]. Quantum interference therefore becomes as important in quantum percolation as the existence of the connection between the vertices, making it a more intriguing setting when compared to the classical percolation [11–14].

Transport of a two-state quantum system across a large network is an important process in quantum information processing and communication protocols [15] and by today many physical systems are tested for their scalability and engineering properties. Furthermore, in last couple of years quantum transport models have also shown a certain applicability to understanding transport processes in biological and chemical systems [16, 17]. Since these natural or synthetic systems are not guaranteed to have a perfectly connected lattice structure, it is important to consider the possible role quantum percolation can play in understanding transport in these systems. To model the dynamics of the quantum particle we choose the process of quantum walks, which in recent years have been shown to be an important and highly applicable mechanism [18]. Recently, first studies on quantum walks in percolating graphs have been reported for circular and linear geometries [19] and for square lattices using a four-state particle [20].

Here we present a new model of a directed discrete-time quantum walk (D-DQW) to study quantum percolation of a two-state particle on a two-dimensional (2D) lattices. The D-DQW is a physically relevant model which, for example, describes the dynamics of transverse propagation of electrons and photons in 2D lattices and optical waveguides. Our main finding is that the possible localisation due to quantum interference at disconnected vertices leads to an Anderson transition point (p_a) which differs significantly from its classical counterpart. To show this we consider three lattice geometries (square lattice, honeycomb lattice and nanotube geometry) and numerically determine p_a for different lattice sizes. We also show that generalising the D-DQW dynamics to allow for more degrees of freedom results in the same values for p_a, hinting at the significance of D-DQW as a fundamental and efficient model to describe dynamics. Interestingly, we find that p_a is lattice size dependent and tends towards unity for larger lattices. This is in contrast to the classical case, where the percolation threshold is independent of the lattice size. We also find that p_a is smaller for finite size honeycomb lattices and the nanotube geometry when compared to the square lattice.

This model can effectively be used as a framework to explore the dynamics for different evolution protocols and

find the most suitable model to describe the quantum transport in various natural physical systems. For engineered systems one can explore the dynamical processes for given lattice structures of different size which might have a large degree of disconnected vertices and test their suitability for quantum information storage or quantum communication protocols.

Model - Let us first define the dynamics of a D-DQW on a completely connected square lattice. The Hilbert space of the particle, $\mathcal{H}_P$, is represented by its internal states, $|\downarrow\rangle = \begin{bmatrix}1\\0\end{bmatrix}$ and $|\uparrow\rangle = \begin{bmatrix}0\\1\end{bmatrix}$ and the Hilbert space of the square lattice of dimension $n \times n$, $\mathcal{H}_L$, is represented by the position of the vertices, $|x, y\rangle$. Each step of the walk consists of first evolving the particle into a superposition of the internal states using a coin flip operation W_θ followed by the shift in the x and y directions using W_x^c and W_y^c, respectively. The index c stands for completely connected vertices in the lattice. The W_θ and W_x^c are the same operations as used in the standard 1D DQW [21–23],

$$W_\theta \equiv \begin{bmatrix} \cos(\theta) & -i\sin(\theta) \\ -i\sin(\theta) & \cos(\theta) \end{bmatrix} \otimes |x,y\rangle\langle x,y|, \quad (1)$$

$$W_x^c \equiv \sum_x \sum_y \Big[|\downarrow\rangle\langle\downarrow| \otimes |x-1,y\rangle\langle x,y| + |\uparrow\rangle\langle\uparrow| \otimes |x+1,y\rangle\langle x,y| \Big]. \quad (2)$$

For the shift in y-direction, we define the position dependent basis states $|-_{x,y}\rangle = \beta^*_{x,y}|\downarrow\rangle - \alpha^*_{x,y}|\uparrow\rangle$ and $|+_{x,y}\rangle = \alpha_{x,y}|\downarrow\rangle + \beta_{x,y}|\uparrow\rangle$, so that

$$W_y^c \equiv \sum_x \sum_y \Big[|-_{x,y-1}\rangle\langle -_{x,y}| \otimes |x,y-1\rangle\langle x,y| + |+_{x,y+1}\rangle\langle +_{x,y}| \otimes |x,y+1\rangle\langle x,y| \Big], \quad (3)$$

where $\alpha_{x,y} = \alpha_{x+1,y}$ and $\beta_{x,y} = \beta_{x-1,y}$ to ensure transport in the positive y-direction only. The state of the particle after t steps is then given by

$$|\Psi_t\rangle = [W_y^c W_x^c W_\theta]^t |\Psi_{in}\rangle = \sum_x \sum_y |\psi_{x,y}\rangle, \quad (4)$$

and we assume the initial state to be $|\Psi_{in}\rangle = \big(\cos(\delta/2)|\downarrow\rangle + e^{i\eta}\sin(\delta/2)|\uparrow\rangle\big) \otimes |\lfloor n/2\rfloor, 1\rangle$ [24] and $|\psi_{x,y}\rangle = (\alpha_{x,y}|\downarrow\rangle + \beta_{x,y}|\uparrow\rangle) \otimes |x,y\rangle = \psi^\downarrow_{x,y} + \psi^\uparrow_{x,y}$.

In Fig. 1(a), we show the path taken by a particle on a perfectly connected square lattice. The probability of detecting the particle outside of the lattice after t steps is given by,

$$P(t) = 1 - \sum_x \sum_y \langle x,y|\rho(t)|x,y\rangle, \quad (5)$$

where $\rho(t) = |\Psi_t\rangle\langle\Psi_t|$. Note that due to the directed component of the walk one finds $P(t) = 1$ for $t > n$.

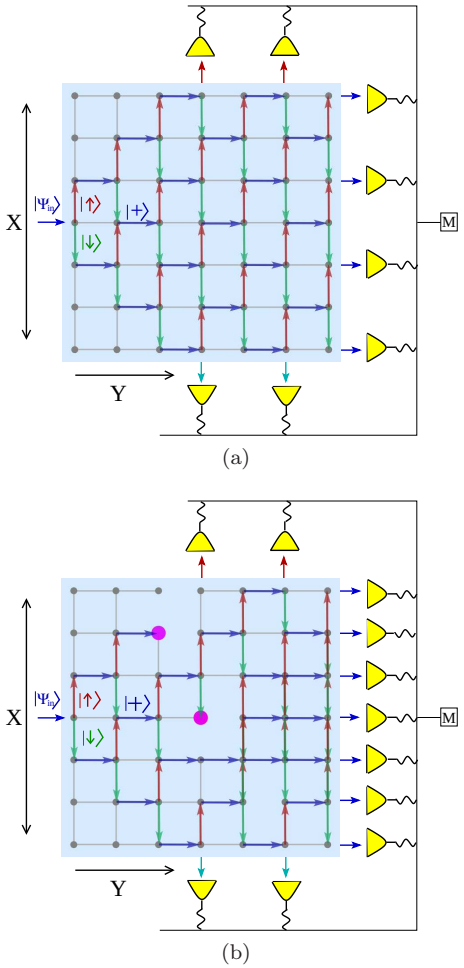

FIG. 1: **Schematic of the path taken by a two-state particle on a square lattice**. Green, red and blue arrows represent the direction of $|\downarrow\rangle$, $|\uparrow\rangle$ and both the states, respectively, when **(a)** all vertices are perfectly connected and **(b)** some connections are missing leading to localization at the highlighted positions.

An alternative description of this dynamics can be found in the form of a differential equation by considering the state of the particle at vertex (x, y) as a function of θ at any time t,

$$\psi^\downarrow_{x,y} = \cos(\theta)\psi^\downarrow_{x+1,y-1} - i\sin(\theta)\psi^\uparrow_{x-1,y-1} \quad (6)$$

$$\psi^\uparrow_{x,y} = \cos(\theta)\psi^\uparrow_{x-1,y-1} - i\sin(\theta)\psi^\downarrow_{x+1,y-1}\,. \quad (7)$$

These equations can be easily decoupled and written as,

$$\psi^{\downarrow(\uparrow)}_{x,y+1} + \psi^{\downarrow(\uparrow)}_{x,y-1} = \cos(\theta)\left[\psi^{\downarrow(\uparrow)}_{x-1,y} + \psi^{\downarrow(\uparrow)}_{x+1,y}\right]. \quad (8)$$

Subtracting then $2\,[1+\cos(\theta)]\,\psi^{\downarrow(\uparrow)}_{x,y}$ from both sides of Eq. (8), we obtain a difference form which can be written as a second order differential wave equation

$$\left[\frac{\partial^2}{\partial y^2} - \cos(\theta)\frac{\partial^2}{\partial x^2} + 2[1-\cos(\theta)]\right]\psi^{\downarrow(\uparrow)}_{x,y} = 0. \quad (9)$$

One can see that the wave-packet propagates along both directions on the x-axis at a rate of $D_x = |\sqrt{\cos(\theta)}|$ per

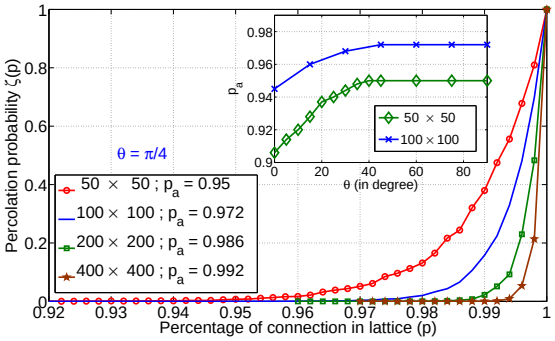

FIG. 2: **Increase in the percolation probability and the Anderson transition point as a function of the percentage of connections, the lattice size and the coin parameter θ.** Probability for a particle to be found outside of the square lattice as a function of the percentage of connected vertices for different lattice sizes for $\theta = \pi/4$. The Anderson transition point can be seen to approach unity for increasing lattice size and also has a strong dependence on θ for $\theta < \pi/4$ (see inset).

time step [25] and in the positive y direction at the rate of $D_y = 1$. For a completely connected lattice the total displacement after time t in the x- and the y-direction will therefore be $D_x(t) = |t\sqrt{\cos(\theta)}|$ and $D_y(t) = t$, respectively.

Let us now consider lattice structures in which some of the edges connecting the vertices are missing. If all edges connecting the vertices on the lattice can be represented by a set E, the shift operator along the x- and y-axis can be written as

$$W_x = \begin{cases} W_x^c & \text{if } \Big(\{x,y\},\{x+1,y\}\Big) \\ & \text{and } \Big(\{x,y\},\{x-1,y\}\Big) \in E \\ W_x^d & \text{otherwise} \end{cases} \tag{10}$$

$$W_y = \begin{cases} W_y^c & \text{if } \Big(\{x,y\},\{x,y+1\}\Big) \in E \\ W_y^d & \text{otherwise} \end{cases} \tag{11}$$

where W_x^c and W_y^c are given in Eqs. (2) and (3), and

$$W_x^d \equiv \sum_{x,y} \Big[(|\downarrow\rangle\langle\downarrow| + |\uparrow\rangle\langle\uparrow|) \otimes |x,y\rangle\langle x,y| \Big] \tag{12}$$

$$W_y^d \equiv \sum_{x,y} \Big[(|-_{x,y}\rangle\langle -_{x,y}| + |+_{x,y}\rangle\langle +_{x,y}|) \otimes |x,y\rangle\langle x,y| \Big]. \tag{13}$$

Here the index d stand for vertices with disconnected edges. In Fig. 1(b), we show an example of a path taken by a particle in a lattice where some connections are missing. In a classical setting the percolation threshold for this square lattice can be calculated to be $p_c = 0.5$ and is known to be independent of the lattice size. In a quantum system, however, a disconnected vertex breaks the well defined interference of the multiple traversing paths and results in trapping a fraction of the amplitude at the disconnected vertex. This mix up of the interference due to the disorder is known to result in Anderson localization [5, 6] and consequently a large percentage of connected vertices are required to reach a non-zero probability for the particle to cross the lattice. In the following we will call the probability for the particle to cross the lattice the percolation probability, $\zeta(p)$, and its critical value at which the percentage of connected vertices p is large enough to reach $\zeta(p) = 0.01$ the Anderson transition point, p_a. It is obtained numerically by averaging over several runs and one of our main findings is that it is significantly larger than p_c for the same lattice. We also find that it converges towards unity with increasing lattice size. To show this we plot the average $\zeta(p)$ as a function of p for square lattices of different size in Fig. 2.

When all vertices in the square lattice are fully connected, initial position $(x,y) = (\lfloor n/2 \rceil, 1)$ and $\theta = 0$, the two basis states move away from each other along the x-axis (no interference takes place) and exit from the sides when half way through the y-axis. For finite values of θ, the exit point is pushed towards the positive y direction due to interference in both directions along the x-axis. In the absence of perfect connections between the vertices in a lattice of finite size, the paths are altered resulting in interference for all values of θ. For small values of θ however, a large fraction of the states still exits along the sides without interference and therefore only a smaller number of connections play a role. This explains the increase in p_a as a function of θ and to show this we plot p_a as function of θ in the inset of Fig. 2. For large lattice size, dependence of p_a on θ will be negligible.

In the same way as for Eq. (9), a general differential equation for one step evolution on a lattice with disconnected vertices can be written as [26],

$$\begin{aligned} \Big[& \Big[p^3 + 2p^2(1-p) + p(1-p)^2\Big]\frac{\partial^2}{\partial y^2} \\ & - \Big[p^3 - p^2(1-p)\Big]\cos(\theta)\frac{\partial^2}{\partial x^2} - 2p^2(1-p)\Big[\cos(\theta)\frac{\partial}{\partial x} + \frac{\partial}{\partial y}\Big] \\ & + [1-\cos(\theta)]\Big[2p^3 + 5p^2(1-p) + 8p(1-p)^2 + 2(1-p)^3\Big] \\ & + p^2(1-p)[1-3\cos(\theta)]\Big]\psi^{\uparrow}_{x,y} = 0. \end{aligned} \tag{14}$$

When $p = 1$ the expression reduces to Eq. (9) and when $p = 0$ all the derivative terms vanish. Here the terms containing the first and second order derivatives contribute to the propagation and the other terms describe localization. Even for values of $p \to 1$ one can see the dominance of the non-derivative terms, which explains the large value for p_a.

Generic extension: The assumption of having the same coin operator at each lattice site is a rather strong one and in the following we will relax this condition to account for applications in more realistic situations. For this we replace θ by a vertex dependent parameter,

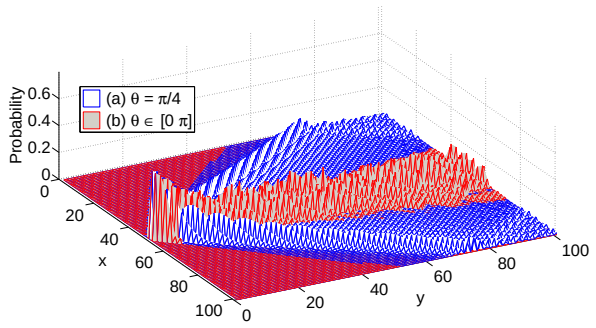

FIG. 3: **Smaller spread in probability distribution for the D-DQW for $\theta_{x,y}$ when compared with $\theta = \pi/4$.** Spread in the probability distribution in x-direction during propagation in the y-direction for a particle walking on a completely connected square lattice of size 100×100. In (a) $\theta = \pi/4$ is used for each step of the D-DQW and in (b) the coin is position dependent, $\theta_{x,y} \in [0, \pi]$. The smaller spread in x direction for $\theta_{x,y}$ is clearly visible (red).

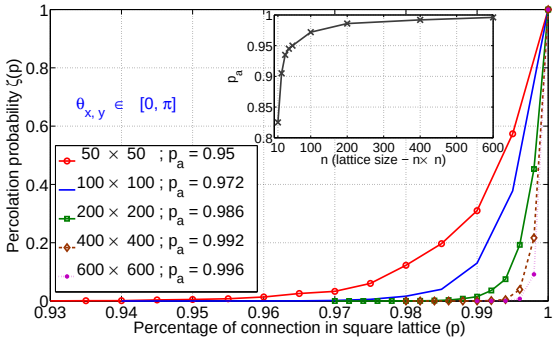

FIG. 4: **Increase in percolation probability and Anderson transition point as a function of the percentage of connections and the lattice size.** Percolation probability as a function of the percentage of connected vertices for square lattices of different size. Each vertex has a different value of $\theta_{x,y}$, which has been randomly chosen from $[0, \pi]$. The p_a shifts towards unity with increasing lattice size (see inset).

$\theta_{x,y} \in [0, \pi]$ and note that $\cos(\theta_{x,y})$ will be negative for any $\theta_{x,y} \in [\pi/2, \pi]$. This can be interpreted as the displacement of the left moving component to the right and the right moving component to the left along the x-direction, which in turn can lead to localization in transverse direction [27]. We show this in Fig. 3, where a typical probability distribution of the particle in x-direction during its propagation in y-direction on a completely connected square lattice for a single realization. The average percolation probability as a function of p for this evolution is then shown in Fig. 4 and, interestingly, we find that the disorder in the form $\theta_{x,y}$ does not result in any noticeable change in the value of p_a when compared to $\theta = \pi/4$. This is due to nearly the same degree of interference [27] for both $\theta_{x,y}$ and $\theta = \pi/4$ and highlights the dominance of the localization effects on disconnect vertices. This can also be seen from Eq. (14), where replacing θ with $\theta_{x,y}$ will not result in significant change in the dynamics due to the dominance of p for $p < 1$.

Quantum percolation on a honeycomb lattice and nanotubes- Transport processes on honeycomb lattices and nanotubes have attracted considerable attention in recent years [28] and the two-state quantum percolation model can be expected to give useful insight into the behaviour of quantum currents and their transition points. In Fig. 5, we show the path taken by the two-state D-DQW on the honeycomb lattice of dimension 9×9. Each step of D-DQW now comprises of the sequence $W_y W_q W_\theta$, where the quantum coin operator W_θ and the operator for the directed evolution in the y-direction, W_y, are same ones as used for the evolution on square lattice. Due to the honeycomb geometry, the transition W_q from q to $q \pm 1$ corresponds to a shift along two edges, first in the $\pm x$ direction and then along the positive y direction. In Fig. 6(a) we show the average percolation probability as a function of the percentage of connected vertices with

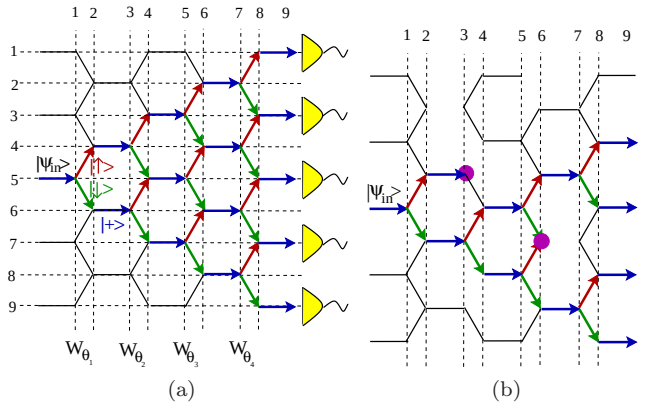

FIG. 5: **Schematic of the path taken by a two state particle on a honeycomb lattice.** D-DQW on an honeycomb lattice of dimension 9×9, where (a) shows the situation where all connections between the vertices are present and (b) the situation where a finite number of connections are missing. This leads to localization at the marked position. Red and green represents the path taken by the two internal states and blue represent the path taken by both the states.

randomly assigned value of $\theta_{x,y} \in [0, \pi]$. Similarly to the square lattice we find that the Anderson transition point p_a is significantly larger than the classical percolation threshold $p_c = 0.652$ [29] and also lattice size dependent. Note that compared to a square lattice of the same size, p_a for honeycomb lattice is smaller, which gives the honeycomb structure a edge over the square lattice for quantum percolation using D-DQW. This is the reversed situation compared to the classical scenario. This can be understood by considering the geometry of the honeycomb lattice: the particle needs to only propagate along two edges to shift one position in x direction and two positions in y direction, whereas in the square lattice transport along three edges is necessary to achieve this.

A natural extension of the honeycomb lattice is to

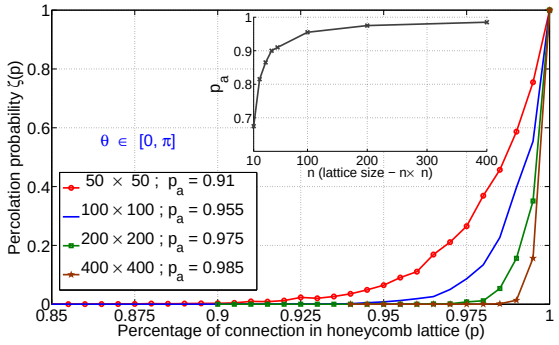

(a)

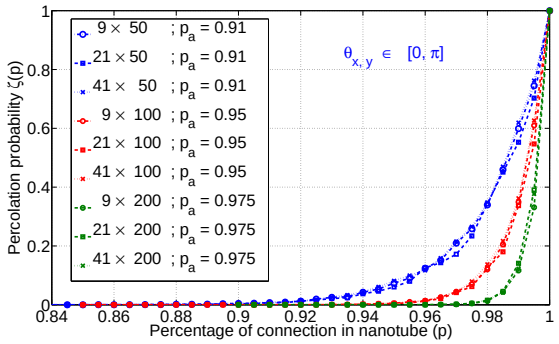

(b)

FIG. 6: **Increase in percolation probability and Anderson transition point for a honeycomb lattice and a nanotube geometry.** Percolation probability as a function of percentage of connected vertices for (a) honeycomb lattices and (b) nanotube structures of different sizes. For the particle transport process the value of θ has been randomly assigned from $[0, \pi]$ for each vertex. With increase in lattice size, p_a shifts towards unity. For nanotubes of size $n \times y$ the transition point can be seen to be independent of n

consider periodic boundary conditions in the x-direction, which transforms the honeycomb lattice into a nanotube geometry. This corresponds to transitions from q to $(q \pm 1 \bmod n)$, where n is the number of vertices along the x-axis and in Fig. 6(b) we show the percolation probability for such a structure as a function of the percentage of connected vertices with randomly assigned values of $\theta_{x,y} \in [0, \pi]$ at each vertex. One can see that the Anderson transition point is same as that to the flat honeycomb structure with same number of edges in the transverse direction, which can be understood by realising that the periodic boundary conditions make the particle encounter the the disconnected vertices more than once. The nanotube with small number of vertices in radial direction therefore corresponds to an effectively larger flat system with the same defect density and from the earlier studies we know that larger lattices have higher Anderson transition points. Due to the absence of the exit point along the radial axis, the only direction the particle can exit is the positive y-direction, which explains the independence of p_a from the number of radial vertices. To summarise

TABLE I: Anderson transition point for finite systems.

Size	Square	Honeycomb	Size (n = 9, 21, 41)	Nanotube
50×50	0.95	0.91	$n \times 50$	0.91
100×100	0.972	0.955	$n \times 100$	0.95
200×200	0.986	0.975	$n \times 200$	0.975
400×400	0.992	0.985	-	-

our main results, we show a comparison of p_a for the different geometries discussed above in Table I.

In conclusion, we have investigated quantum percolation using a directed two-state DQW to model the quantum transport process. We have shown that the transition point p_a, beyond which quantum transport can be seen is relatively large when compared to the classical percolation threshold, p_c. In addition, for finite lattice size and unlike the classical case, we have found that p_a is size dependent and tends towards unity with increase in size. This suggests that even a small disconnected vertices in the large system obstructs the quantum transport.

Comparing different lattice geometries we found that p_a is smaller for honeycomb structures and nanotube geometry as compared to square lattice. This variation suggests that one can explore the dynamics on different lattice structures to find one most suitable for a required purpose. For example, higher p_a can allow for storage and lower ones for more efficient transport processes.

The two-state quantum percolation model using D-DQW for transport process is a realistic model that can be used to study transport process in various directed physical systems such as photon dynamics in waveguides with disconnected paths or quantum currents on nanotubes. We have demonstrated its generality by allowing the parameter θ to vary randomly at each vertex and showed that this does not lead to any significant change in p_a. Given the current experimental interest and advances in implementing quantum walks in various physical systems [30], we believe that our discrete model is a strong candidate for upcoming experimental studies and its differential equation form we have presented will also be interest for further theoretical analysis.

* Electronic address: c.madaiah@oist.jp
† Electronic address: thomas.busch@oist.jp

[1] S. Kirkpatrick, Rev. Mod. Phys. **45**, 574 - 588 (1973); B. Bollobás, *et al.*, Percolation, Cambridge University Press (2006).
[2] M. Sahini and M. Sahimi, *Applications Of Percolation Theory*, CRC Press (1994).
[3] K. Kieling and J. Eisert, *Percolation in Quantum Computation and Communication* in Quantum and Semi-classical Percolation and Breakdown in Disordered Solids, pages 287-319 (Springer, Berlin, 2009).

[4] D. Stauffer and A. Aharony, Introduction to Percolation Theory (2nd ed.), CRC Press (1994).
[5] P. W. Anderson, Phys. Rev. **109**, 1492 (1958).
[6] P. A. Lee and T. V. Ramakrishnan, Rev. Mod. Phys. **57**, 287 (1985).
[7] F. Evers and A. D. Mirlin, Rev. Mod. Phys. **80**, 1355 (2008).
[8] T. Schwartz, G. Bartal, S. Fishman, and M Segev, Nature **446**, 52 - 55 (1 March 2007).
[9] J. Chabé, G. Lemarié, B. Grémaud, D. Delande, P. Szriftgiser, and J. C. Garreau, Phys. Rev. Lett. **101**, 255702 (2008).
[10] A. Crespi, R. Osellame, R. Ramponi, V. Giovannetti, R. Fazio, L. Sansoni, F. De Nicola, F. Sciarrino, and P. Mataloni, Nature Photonics (2013), doi:10.1038/nphoton.2013.26.
[11] D. Vollhardt and P. Wölfle. In: Electronic Phase Transitions, ed by W. Hanke and Y. V. Kopaev, p. 1 (North Holland, Amsterdam, 1992).
[12] G. Schubert and H. Fehske, *Quantum and Semi-classical Percolation and Breakdown in Disordered Solids*, Lecture Notes in Physics **762**, 1-28 (2009).
[13] S. Kirkpatrick and T.P. Eggarter, Phys. Rev. B 6, 3598 (1972).
[14] Y. Shapir *et al.*, Phys. Rev. Lett. **49**, 486 (1982).
[15] *Quantum Computation and Quantum Information*M. A. Nielsen (Author), I. L. Chuang, Cambridge University Press (2000).
[16] G. S. Engel *et al.*, Nature **446**, 782-786 (2007).
[17] M. Mohseni *et al.*, J. Chem. Phys. **129**, 174106 (2008) ; M.B. Plenio and S.F. Huelga, New J. Phys. **10**, 113019 (2008).
[18] Salvador E. Venegas-Andraca, Quantum Information Processing vol. **11** (5), pp. 1015-1106 (2012).
[19] B. Kollár *et al.*, Phys. Rev. Lett. **108**, 230505 (2012)
[20] G. Leung *et al.*, New J. Phys. **12** 123018 (2010)
[21] G. V. Riazanov, Sov. Phys. JETP **6** 1107 (1958) ; R. Feynman, Found. Phys. **16**, 507 (1986) ; K. R. Parthasarathy, Journal of Applied Probability, **25**, 151-166 (1998).
[22] Y. Aharonov *et al.*, Phys. Rev. A **48**, 1687, (1993) ; D. A. Meyer, J. Stat. Phys. **85**, 551 (1996).
[23] C. M. Chandrashekar, R. Srikanth and Raymond Laflamme, Phys. Rev. A, 77, 032326 (2008).
[24] For the numerical simulation we have used $\delta = \eta = 0$, but our conclusion are independent of the initial states of the particle.
[25] C. M. Chandrashekar, S. Banerjee, R. Srikanth, Phys. Rev. A, **81**, 062340 (2010).
[26] The details for the derivation of this expression can be found in the supplementary material.
[27] C. M. Chandrashekar, arXiv: 1212.5984.
[28] S. D. Sarma *et al.* , Rev. Mod. Phys. **83**, 407 - 470 (2011).
[29] M. F. Sykes and J. W. Essam, J. Math. Phys. **5**, 1117 (1964).
[30] J. Du *et al.*, Phys. Rev. A **67**, 042316 (2003) ; C. A. Ryan *et al.*, Phys. Rev. A**72**, 062317 (2005) ; B. Do *et al.*, J. Opt. Soc. Am. B **22**, 499 (2005) ; H. B. Perets *et al.*, Phys. Rev. Lett. **100**, 170506 (2008) ; H. Schmitz *et al.*, Phys. Rev. Lett. **103**, 090504 (2009) ; F. Zahringer *et al.*, Phys. Rev. Lett. **104**, 100503 (2010) ; K. Karski *et al.*, Science **325**, 174 (2009) ; A. Schreiber *et al.*, Phys. Rev. Lett., **104**, 05502 (2010) ; M. A. Broome *et al.*, Phys. Rev. Lett. **104**, 153602 (2010) ; A. Peruzzo *et al.*, Science **329**, 1500 (2010) ; L. Sansoni *et al.*, Phys. Rev. Lett. **108**, 010502 (2012).

SUPPLEMENTARY MATERIAL : QUANTUM PERCOLATION AND ANDERSON TRANSITION POINT FOR TRANSPORT OF A TWO-STATE PARTICLE

For a completely connected lattice, it is straight forward to write the states of the particle at position (x, y) as function of θ at any time t (see Eqs. (6) and (7) in the paper) and obtain a differential equation form. When we have disconnected vertices, we need write down all the possible configurations for the state of the particle at vertex (x, y) with probability of that possibility. For quantum percolation using D-DQW we find that the eight possible configuration can effectively describe the dynamics. We obtain the effective differential equation form by summing up the equations for each configuration with their respective probability of the possibility of occurrence.

Stencil and the states for the vertex (x, y)

In Fig. 7, we show the four configurations that result in transport of state from $(x \pm 1, y-1)$ and $(x, y-1)$ to (x, y). In Fig. 8, we show the other four configurations that results in transport of state from $(x \pm 1, y-1)$ to $(x, y-1)$ and the configuration that gets trapped at position $(x, y-1)$. This is equivalent configurations that results in transport of state from $(x \pm 1, y)$ to (x, y) and the configuration that gets trapped at position (x, y).

Figure. 7(a): Completely connected state and the expression are same as Eqs. (6) and (7) in the paper:

$$\psi^{\downarrow}_{x,y} = \cos(\theta)\psi^{\downarrow}_{x+1,y-1} - i\sin(\theta)\psi^{\uparrow}_{x-1,y-1} \tag{15}$$

$$\psi^{\uparrow}_{x,y} = \cos(\theta)\psi^{\uparrow}_{x-1,y-1} - i\sin(\theta)\psi^{\downarrow}_{x+1,y-1}\ . \tag{16}$$

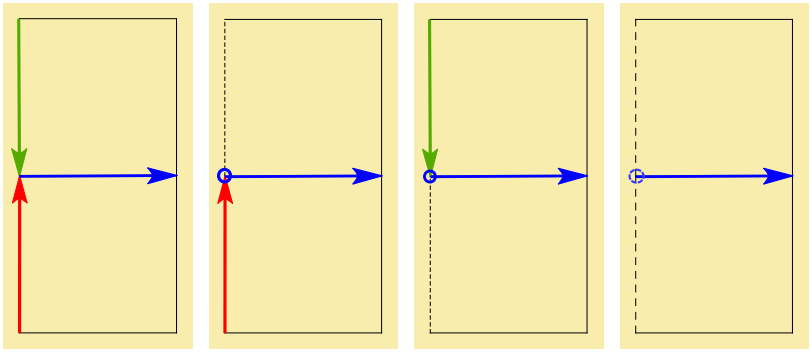

(a) (b) (c) (d)

FIG. 7: (Color online) Four possible configuration when the transport can happen to vertex (x, y). Green, red and blue arrows representing the direction of $|\downarrow\rangle$, $|\uparrow\rangle$ and both the states, respectively. Transport from (a) $(x+1, y-1)$ and $(x-1, y-1)$ to (x, y), (b) $(x-1, y-1)$ and $(x, y-1)$ to (x, y), (c) $(x+1, y-1)$ and $(x, y-1)$ to (x, y) and (d) $(x, y-1)$ to (x, y).

These equations can be easily decoupled and written as,

$$\psi^{\downarrow(\uparrow)}_{x,y+1} + \psi^{\downarrow(\uparrow)}_{x,y-1} = \cos(\theta)\left[\psi^{\downarrow(\uparrow)}_{x-1,y} + \psi^{\downarrow(\uparrow)}_{x+1,y}\right]. \tag{17}$$

Subtracting $2\left[1+\cos(\theta)\right]\psi^{\downarrow(\uparrow)}_{x,y}$ from both sides of the preceding expression, we obtain a difference form which can be written as a second order differential wave equation

$$\left[\frac{\partial^2}{\partial y^2} - \cos(\theta)\frac{\partial^2}{\partial x^2} + 2[1-\cos(\theta)]\right]\psi^{\downarrow(\uparrow)}_{x,y} = 0. \tag{18}$$

When p is the percentage of connection in the lattice the probability for the above possibility is p^3.

Figure. 7(b): Because of the missing edge from vertex $(x, y-1)$ to $(x+1, y-1)$, the state arriving from $(x, y-2)$ will remain in $(x, y-1)$ to which the state from $(x-1, y-1)$ join to proceed further to (x, y). For this configuration the state at (x, y) will be :

$$\psi^{\downarrow}_{x,y} = \cos(\theta)\psi^{\downarrow}_{x,y-1} - i\sin(\theta)\left[\psi^{\uparrow}_{x-1,y-1} + \psi^{\uparrow}_{x,y-1}\right] \tag{19}$$

$$\psi^{\uparrow}_{x,y} = -i\sin(\theta)\psi^{\downarrow}_{x,y-1} + \cos(\theta)\left[\psi^{\uparrow}_{x-1,y-1} + \psi^{\uparrow}_{x,y-1}\right]. \tag{20}$$

After decoupling we get

$$\psi^{\uparrow}_{x,y+1} + \psi^{\uparrow}_{x,y-1} - \cos(\theta)\psi^{\uparrow}_{x-1,y} + \psi^{\uparrow}_{x-1,y-1} = 2\cos(\theta)\psi^{\uparrow}_{x,y}. \tag{21}$$

Subtracting both sides of the preceding expression by $[2+\cos(\theta)]\psi^{\uparrow}_{x,y} + \psi^{\uparrow}_{x+1,y}$ we obtain a difference form which can be written as

$$\left[\frac{\partial^2}{\partial y^2} + \cos(\theta)\frac{\partial}{\partial x} + [2-3\cos(\theta)]\right]\psi^{\uparrow}_{x,y} = \left[\frac{\partial}{\partial y} - 1\right]\psi^{\uparrow}_{x-1,y}. \tag{22}$$

The right hand side can be further simplified to obtain

$$\left[\frac{\partial^2}{\partial y^2} + \frac{\partial^2}{\partial y \partial x} + [1-\cos(\theta)]\frac{\partial}{\partial x} - \frac{\partial}{\partial y} + 3[1-\cos(\theta)]\right]\psi^{\uparrow}_{x,y} = 0. \tag{23}$$

The probability for the above possibility is $p^2(1-p)$.

Figure. 7(c): For this configuration the state at (x, y) will be :

$$\psi^{\downarrow}_{x,y} = \cos(\theta)\left[\psi^{\downarrow}_{x,y-1} + \psi^{\downarrow}_{x+1,y-1}\right] - i\sin(\theta)\psi^{\uparrow}_{x,y-1} \tag{24}$$

$$\psi^{\uparrow}_{x,y} = i\sin(\theta)\left[\psi^{\downarrow}_{x,y-1} + \psi^{\downarrow}_{x+1,y-1}\right] + \cos(\theta)\psi^{\uparrow}_{x,y-1}. \tag{25}$$

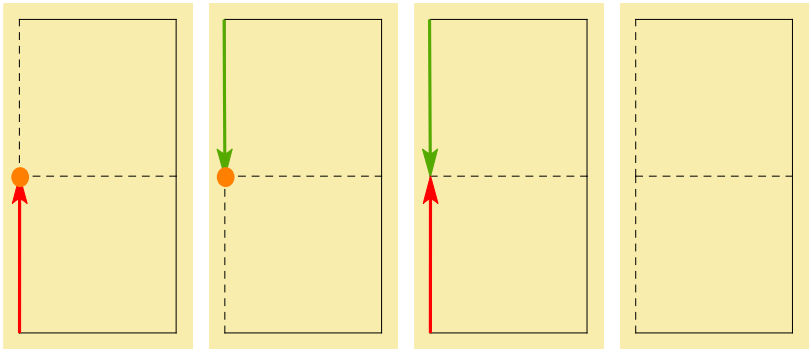

(a) (b) (c) (d)

FIG. 8: (Color online) During the transport the state from (a) $(x-1, y-1)$ gets trapped at $(x, y-1)$ and (b) $(x+1, y-1)$ gets trapped at $(x, y-1)$. (c) Due to the absence of edge from $(x, y-1)$ to (x, y) the states from $(x \pm 1, y)$ move back to $(x, \pm 1, y)$. (d) absence of any transport or trapping.

After decoupling we get

$$\psi^{\uparrow}_{x,y+1} + \psi^{\uparrow}_{x,y-1} - \cos(\theta)\psi^{\uparrow}_{x+1,y} + \psi^{\uparrow}_{x+1,y-1} = 2\cos(\theta)\psi^{\uparrow}_{x,y}. \tag{26}$$

Subtracting both sides of the preceding expression by $[2+\cos(\theta)]\psi^{\uparrow}_{x,y} + \psi^{\uparrow}_{x-1,y}$ we obtain a difference form which can be written as

$$\left[\frac{\partial^2}{\partial y^2} - \cos(\theta)\frac{\partial}{\partial x} + [2 - 3\cos(\theta)]\right]\psi^{\uparrow}_{x,y} = \left[\frac{\partial}{\partial y} - 1\right]\psi^{\uparrow}_{x+1,y}. \tag{27}$$

The right hand side can be further simplified to obtain

$$\left[\frac{\partial^2}{\partial y^2} - \frac{\partial^2}{\partial y \partial x} - [1+\cos(\theta)]\frac{\partial}{\partial x} - \frac{\partial}{\partial y} + [1 - 3\cos(\theta)]\right]\psi^{\uparrow}_{x,y} = 0. \tag{28}$$

The probability for the above possibility is $p^2(1-p)$.

Figure. 7(d):

$$\psi^{\downarrow}_{x,y} = \cos(\theta)\psi^{\downarrow}_{x,y-1} - i\sin(\theta)\psi^{\uparrow}_{x,y-1} \tag{29}$$

$$\psi^{\uparrow}_{x,y} = -i\sin(\theta)\psi^{\downarrow}_{x,y-1} + \cos(\theta)\psi^{\uparrow}_{x,y-1}. \tag{30}$$

After decoupling we get

$$\psi^{\uparrow(\downarrow)}_{x,y+1} + \psi^{\uparrow(\downarrow)}_{x,y-1} = 2\cos(\theta)\psi^{\uparrow(\downarrow)}_{x,y}. \tag{31}$$

Subtracting both the sides by $2\psi^{\uparrow(\downarrow)}_{x,y}$ and writing the difference form as a differential equation,

$$\left[\frac{\partial^2}{\partial y^2} + 2\left[1 - \cos(\theta)\right]\right]\psi^{\uparrow(\downarrow)}_{x,y} = 0. \tag{32}$$

The probability for the above possibility is $p(1-p)^2$.

Figure. 8(a):

$$\psi^{\downarrow}_{x,y-1} = \cos(\theta)\psi^{\downarrow}_{x,y-1} - i\sin(\theta)\left[\psi^{\uparrow}_{x-1,y-1} + \psi^{\uparrow}_{x,y-1}\right] \tag{33}$$

$$\psi^{\uparrow}_{x,y-1} = -i\sin(\theta)\psi^{\downarrow}_{x,y-1} + \cos(\theta)\left[\psi^{\uparrow}_{x-1,y-1} + \psi^{\uparrow}_{x,y-1}\right]. \tag{34}$$

which is equivalent to

$$\psi^{\downarrow}_{x,y} = \cos(\theta)\psi^{\downarrow}_{x,y} - i\sin(\theta)\Big[\psi^{\uparrow}_{x-1,y} + \psi^{\uparrow}_{x,y}\Big] \tag{35}$$

$$\psi^{\uparrow}_{x,y} = -i\sin(\theta)\psi^{\downarrow}_{x,y} + \cos(\theta)\Big[\psi^{\uparrow}_{x-1,y} + \psi^{\uparrow}_{x,y}\Big]. \tag{36}$$

After decoupling we get

$$2[1-\cos(\theta)]\psi^{\uparrow}_{x,y} = [\cos(\theta)-1]\psi^{\uparrow}_{x-1,y}. \tag{37}$$

Subtracting both sides of the expression by $[\cos(\theta)-1]\psi^{\uparrow}_{x,y}$ we get a difference form that can be written in the differential equation for as,

$$[1-\cos(\theta)]\Big[3 - \frac{\partial}{\partial x}\Big]\psi^{\uparrow}_{x,y} = 0 \tag{38}$$

The probability for the above possibility is $p(1-p)^2$.

Figure. 8(b):

$$\psi^{\downarrow}_{x,y-1} = \cos(\theta)\Big[\psi^{\downarrow}_{x,y-1} + \psi^{\downarrow}_{x+1,y-1}\Big] - i\sin(\theta)\psi^{\uparrow}_{x,y-1} \tag{39}$$

$$\psi^{\uparrow}_{x,y-1} = -i\sin(\theta)\Big[\psi^{\downarrow}_{x,y-1} + \psi^{\downarrow}_{x+1,y-1}\Big] + \cos(\theta)\psi^{\uparrow}_{x,y-1} \tag{40}$$

$$\tag{41}$$

which is equivalent to

$$\psi^{\downarrow}_{x,y} = \cos(\theta)\Big[\psi^{\downarrow}_{x,y} + \psi^{\downarrow}_{x+1,y}\Big] - i\sin(\theta)\psi^{\uparrow}_{x,y} \tag{42}$$

$$\psi^{\uparrow}_{x,y} = -i\sin(\theta)\Big[\psi^{\downarrow}_{x,y} + \psi^{\downarrow}_{x+1,y}\Big] + \cos(\theta)\psi^{\uparrow}_{x,y} \tag{43}$$

$$\tag{44}$$

After decoupling we get

$$2[1-\cos(\theta)]\psi^{\uparrow}_{x,y} = [\cos(\theta)-1]\psi^{\uparrow}_{x+1,y}. \tag{45}$$

Subtracting both sides of the expression by $[\cos(\theta)-1]\psi^{\uparrow}_{x,y}$ we get a difference form that can be written in the differential equation for as,

$$[1-\cos(\theta)]\Big[3 + \frac{\partial}{\partial x}\Big]\psi^{\uparrow}_{x,y} = 0 \tag{46}$$

The probability for the above possibility is $p(1-p)^2$.

Figure. 8(c):

$$\psi^{\downarrow}_{x,y-1} = \cos(\theta)\psi^{\downarrow}_{x+1,y-1} - i\sin(\theta)\psi^{\uparrow}_{x-1,y-1} \tag{47}$$

$$\psi^{\uparrow}_{x,y-1} = \cos(\theta)\psi^{\uparrow}_{x-1,y-1} - i\sin(\theta)\psi^{\downarrow}_{x+1,y-1}\ . \tag{48}$$

which is equivalent to

$$\psi^{\downarrow}_{x,y} = \cos(\theta)\psi^{\downarrow}_{x+1,y} - i\sin(\theta)\psi^{\uparrow}_{x-1,y} \tag{49}$$

$$\psi^{\uparrow}_{x,y} = \cos(\theta)\psi^{\uparrow}_{x-1,y} - i\sin(\theta)\psi^{\downarrow}_{x+1,y}\ . \tag{50}$$

After decoupling we get

$$2\psi^{\uparrow(\downarrow)}_{x,y} = \cos(\theta)\Big[\psi^{\uparrow(\downarrow)}_{x-1,y} + \psi^{\uparrow(\downarrow)}_{x+1,y}\Big] \tag{51}$$

Subtracting both sides of the preceding expression by $2\cos(\theta)\psi^{\uparrow(\downarrow)}_{x,y}$ and by writing the difference form to the differential equation form we get:

$$\Big[\cos(\theta)\frac{\partial^2}{\partial x^2} - 2[\cos(\theta)-1]\Big]\psi^{\uparrow(\downarrow)}_{x,y} = 0. \tag{52}$$

The probability for the above possibility is $p^2(1-p)$.

Figure. 8(d):

$$\psi^{\downarrow}_{x,y-1} = \cos(\theta)\psi^{\downarrow}_{x,y-1} - i\sin(\theta)\psi^{\uparrow}_{x,y-1} \tag{53}$$
$$\psi^{\uparrow}_{x,y-1} = -i\sin(\theta)\psi^{\downarrow}_{x,y-1} + \cos(\theta)\psi^{\uparrow}_{x,y-1}. \tag{54}$$

which is equivalent to

$$\psi^{\downarrow}_{x,y} = \cos(\theta)\psi^{\downarrow}_{x,y} - i\sin(\theta)\psi^{\uparrow}_{x,y} \tag{55}$$
$$\psi^{\uparrow}_{x,y} = -i\sin(\theta)\psi^{\downarrow}_{x,y} + \cos(\theta)\psi^{\uparrow}_{x,y}. \tag{56}$$

These expressions can be decoupled and written as:

$$2[1-\cos(\theta)]\psi^{\uparrow(\downarrow)}_{x,y} = 0. \tag{57}$$

The probability for the above possibility is $(1-p)^3$.

Adding up the differential equations for all eight configuration as a product of the probability of its possibility we get :

$$\Bigg[\Big[p^3 + 2p^2(1-p) + p(1-p)^2\Big]\frac{\partial^2}{\partial y^2} - \Big[p^3 - p^2(1-p)\Big]\cos(\theta)\frac{\partial^2}{\partial x^2} - 2p^2(1-p)\Big[\cos(\theta)\frac{\partial}{\partial x} + \frac{\partial}{\partial y}\Big]$$
$$+[1-\cos(\theta)]\Big[2p^3 + 5p^2(1-p) + 8p(1-p)^2 + 2(1-p)^3\Big] + p^2(1-p)[1-3\cos(\theta)]\Bigg]\psi^{\uparrow}_{x,y} = 0. \tag{58}$$

Similar expression can be obtained for $\psi^{\downarrow}_{x,y}$.